

# A Conformational Study on Cyclo[(S)-Phenylalanyl-(S)-Histidyl] by Molecular Modelling and NMR Techniques

Michael North

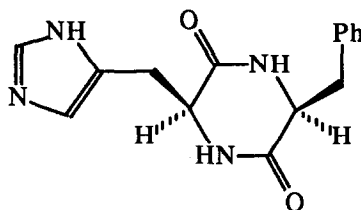
Department of Chemistry, University of Wales, Bangor, Gwynedd, LL57 2UW

(Received in UK 7 May 1992)

**Key Words:** Cyclo[(S)-Phenylalanyl-(S)-Histidyl]; Conformation; Hydrocyanation; Molecular Modelling; NMR

**Abstract:** The conformation of the cyclic dipeptide cyclo[(S)-Phenylalanyl-(S)-Histidyl] is investigated by molecular modelling and NMR techniques. The results are of interest when considering the mechanism by which this compound acts as a catalyst for the asymmetric addition of HCN to aldehydes.

The addition of hydrogen cyanide (or other cyanides) to carbonyl compounds to give cyanohydrins is a well established reaction in organic chemistry<sup>1</sup>. Two aspects of this reaction make it particularly useful, it is a carbon-carbon bond forming reaction and two new functional groups are created during the reaction, allowing the cyanohydrin to be converted into a wide range of other products<sup>2</sup>. The reaction however, has one disadvantage, namely that the cyanohydrins are formed as a racemic mixture thus necessitating a resolution if they are to be used as precursors for biologically active molecules.



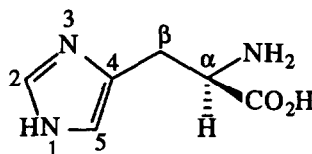
(1)

Recently, a number of compounds have been discovered or designed which catalyse the asymmetric addition of cyanide to aldehydes, giving optically active cyanohydrins. The earliest catalysts were alkaloids<sup>3</sup> and a synthetic polyamine<sup>4</sup> which gave only very low enantiomeric excesses (1 to 20%). Very recently, a series of chiral, metal based Lewis acids have been developed which catalyse the addition of trimethylsilyl cyanide to aldehydes, giving cyanohydrins with moderate to good enantiomeric excesses<sup>5</sup>. However, the most widely studied catalyst for this reaction is the cyclic dipeptide cyclo[(S)-phenylalanyl-(S)-histidyl] (1) which catalyses the addition of hydrogen cyanide to aldehydes with 30-100% ee depending upon the structure of the aldehyde<sup>6-8</sup>. Although a number of papers describing the synthetic utility of this catalyst have appeared<sup>6-8</sup>, very little structural information or mechanistic speculation concerning the cyclic dipeptide (1) is

available<sup>7-9</sup>. A structural and mechanistic investigation of this catalyst and reaction would appear to be justified for the following reasons:-

- 1) The synthetic utility of homochiral cyanohydrins for instance in the preparation of pyrethroids<sup>10</sup>.
- 2) The reaction is an example of a catalytic asymmetric carbon-carbon bond forming reaction, a class of reactions which are still rare but which promise much for the future of asymmetric synthesis.
- 3) An enzyme D-hydroxynitrilase catalyses the same reaction<sup>11</sup>; however, very little is known about the structure of this enzyme. Catalyst (1) is a very good mimic of the enzyme in terms of substrate specificity, product enantiomeric excess and absolute configuration.
- 4) A detailed knowledge of the mode of action of catalyst (1) might allow the design of modified catalysts for this and other reactions such as the addition of HCN to imines and oximes, and the addition of other nucleophiles such as hydrogen azide and 1,3-dicarbonyl compounds to aldehydes.

In this paper a detailed study of the conformation of dipeptide (1) as determined by molecular modelling and NMR techniques is given. Throughout this paper, the various protons and carbons of imidazole will be referred to following IUPAC nomenclature as shown below. Thus the imidazole NH can be either 1H or 3H.



### Molecular Modelling Results

A molecular modelling study of compound (1) was carried out on a Silicon Graphics Personal Iris Workstation using the Macromodel programme<sup>12</sup>. A local minimum energy conformation was first generated by minimising a randomly drawn representation of catalyst (1) using the Amber forcefield and the Truncated Newton-Rapheson Conjugate Gradient minimisation procedure. All freely rotatable bonds, and those in the diketopiperazine ring were then rotated in 60° increments to generate a large number of starting geometries. Those conformations with unreasonable bond lengths (less than 100pm or greater than 200pm) within the diketopiperazine ring were automatically discarded by the programme, and the remainder were minimised as above to generate a set of minimum energy conformations. All conformations within 50kJ mol<sup>-1</sup> of the global minimum energy conformation were stored and evaluated. This procedure was carried out with starting conformers containing both 1H and 3H isomers of the imidazole. These calculations were carried out three times, once with no solvent, and once each with simulated chloroform and water solvents (the only solvents available within Macromodel), and the results are tabulated in Tables 1 to 3.

The following results are immediately apparent. The 3H form of the imidazole is much more stable than the 1H form, so much so that *in vacuo*, and in chloroform, no 1H form has a population above 1%. The reason for this is the presence of an intramolecular hydrogen bond between the imidazole NH and the histidine carbonyl which is only possible in the 3H form. Only in water where hydrogen bonding to solvent can disrupt the intramolecular hydrogen bond is the 1H form populated to a significant extent.

Table 1: Molecular Modelling Results Calculated in Vacuo

Conformer Energy (KJ/Mol)	Population (%) <sup>1</sup>	Imidazole 1H or 3H	Coupling Constants (H <sub>α</sub> -H <sub>β</sub> ) (Hz) <sup>2</sup>		Conformer Type <sup>3</sup>	Diketopiperazine Ring <sup>4</sup>
			His	Phe		
-14.95	46.0	3H	3.4, 2.9	4.0, 2.0	A	F
-14.74	42.3	3H	11.1, 1.6	3.8, 2.7	B	F
-8.2	3.0	3H	3.4, 2.9	11.8, 3.2	D	B
-6.95	1.8	3H	1.8, 1.4	11.8, 2.8	C	B
-6.38	1.4	3H	11.4, 1.8	11.8, 1.3	C	B
-5.22	0.9	3H	11.3, 4.9	4.2, 2.5	B	F

1) Populations are calculated at 298.15K, all conformers with a population of 1% or more are recorded. 2) Coupling constants are calculated within the MacroModel program. 3) Type A has the two aromatic rings facing one another, type B has the imidazole ring pointing out, type C has both aromatic rings pointing outwards, and type D has the benzene ring pointing outwards. 4) F=flat, B=boat.

Table 2: Molecular Modelling Results Calculated in Water

Conformer Energy (KJ/Mol)	Population (%) <sup>1</sup>	Imidazole 1H or 3H	Coupling Constants (H <sub>α</sub> -H <sub>β</sub> ) (Hz) <sup>2</sup>		Conformer Type <sup>3</sup>	Diketopiperazine Ring <sup>4</sup>
			His	Phe		
-149.15	24.3	3H	11.6, 4.2	4.3, 2.4	B	F
-147.60	13.0	3H	3.2, 3.1	4.4, 2.3	A	F
-146.98	10.1	3H	11.8, 3.4	3.9, 2.7	B	F
-146.54	8.5	3H	11.8, 3.1	3.7, 2.8	B	F
-146.30	7.7	3H	3.5, 2.8	3.6, 2.9	A	F
-145.98	6.8	3H	11.7, 3.8	3.3, 3.3	B	F
-145.32	5.2	3H	11.0, 1.5	4.0, 2.6	B	F
-144.85	4.3	1H	11.8, 3.3	3.9, 2.7	B	F
-144.80	4.2	3H	3.2, 3.1	11.8, 2.8	D	F
-144.74	4.1	3H	3.2, 3.1	11.8, 3.0	D	F
-144.05	3.1	3H	3.7, 2.7	11.8, 3.1	C	B
-143.17	2.2	1H	3.6, 2.8	11.8, 2.8	D	F
-142.86	1.9	1H	11.8, 2.9	3.7, 2.9	B	F
-141.51	1.1	1H	3.4, 2.9	3.9, 2.7	A	F
-140.87	0.9	1H	11.8, 3.5	3.7, 2.9	B	F

Footnotes as for Table 1.

The 1H- form is clearly not important when considering this dipeptide in organic solvents *eg* during a hydrocyanation reaction, and will not be considered further. All of the low energy conformations fall into one of four types A-D as shown in Figure 1. Type A is the global minimum in a vacuum, and is U shaped with the two aromatic rings facing one another. The global minimum in chloroform or water however has a different structure (Type B) in which the phenyl ring is bent over the diketopiperazine and the imidazole is pointed outwards. Type C conformations have the same histidine conformation as type B, but have the phenyl ring

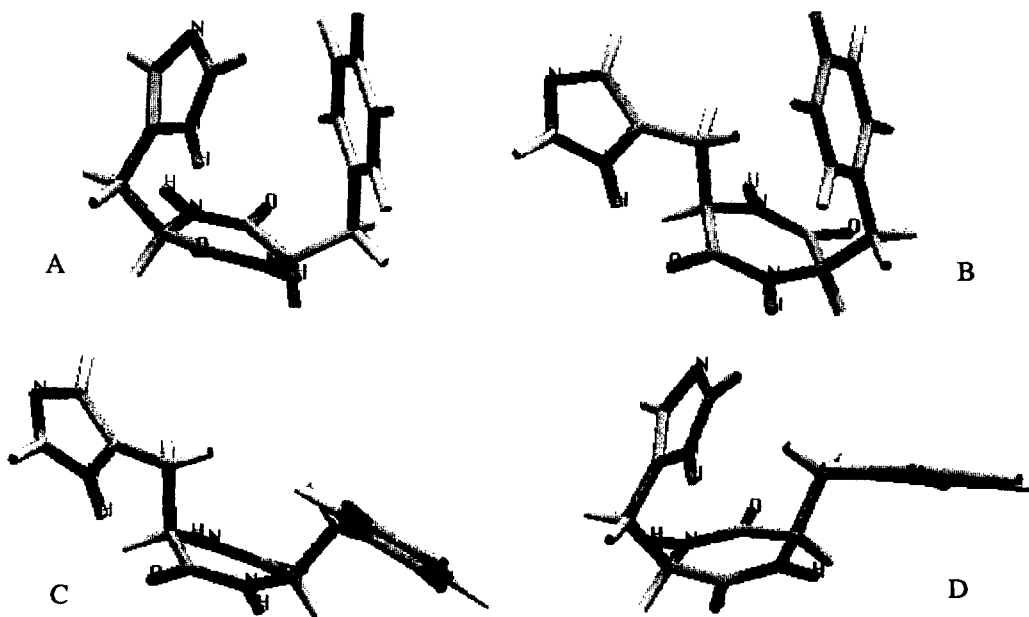
rotated outwards not over the diketopiperazine. Type D is similar to type B except that it is the imidazole that sits over the diketopiperazine, and the phenyl ring that points outwards.

Table 3: Molecular Modelling Results Calculated in Chloroform

Conformer Energy (KJ/Mol)	Population (%) <sup>1</sup>	Imidazole 1H or 3H	Coupling Constants (H <sub>α</sub> -H <sub>β</sub> ) (Hz) <sup>2</sup>		Conformer Type <sup>3</sup>	Diketopiperazine Ring <sup>4</sup>
			His	Phe		
-120.30	28.1	3H	11.0, 1.5	3.9, 2.7	B	F
-119.89	23.8	3H	3.5, 2.9	11.8, 3.2	D	B
-118.97	16.5	3H	11.4, 1.8	11.8, 3.1	C	B
-117.56	9.3	3H	10.9, 1.5	3.5, 3.1	B	F
-117.05	7.6	3H	3.2, 3.1	5.3, 1.7	A	F
-114.39	2.6	3H	3.7, 2.7	5.6, 1.6	A	B
-113.97	2.2	3H	11.0, 1.5	11.7, 3.4	C	B
-113.45	1.8	3H	11.4, 1.8	5.4, 1.7	B	B
-112.81	1.4	3H	11.6, 4.2	3.8, 2.8	B	F
-112.58	1.2	3H	4.1, 2.4	11.8, 3.0	D	F
-112.42	1.2	3H	4.3, 2.2	11.8, 3.2	D	F
-112.22	1.1	3H	11.2, 1.6	4.3, 2.4	B	B
-111.47	0.8	3H	3.2, 3.1	11.8, 3.0	D	F

Footnotes as for table 1.

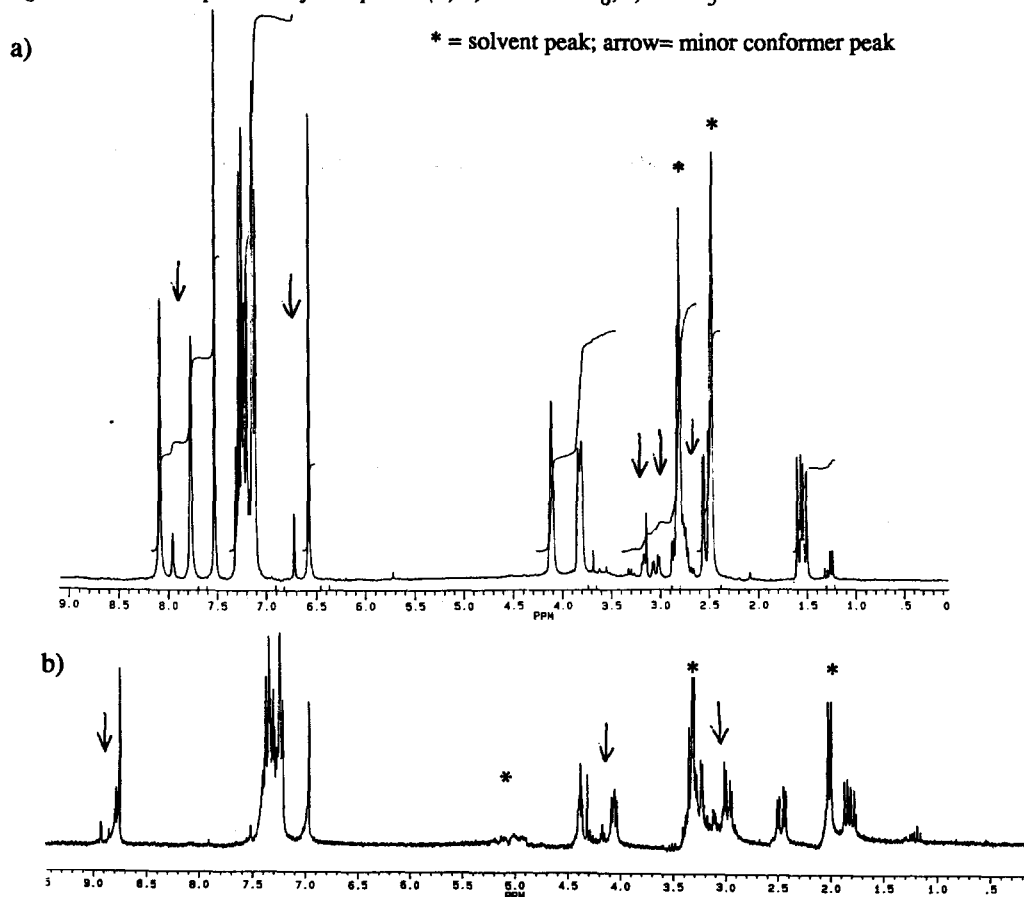
Figure 1: The Four Types of Conformations Found for Dipeptide 1.



### <sup>1</sup>H NMR Results

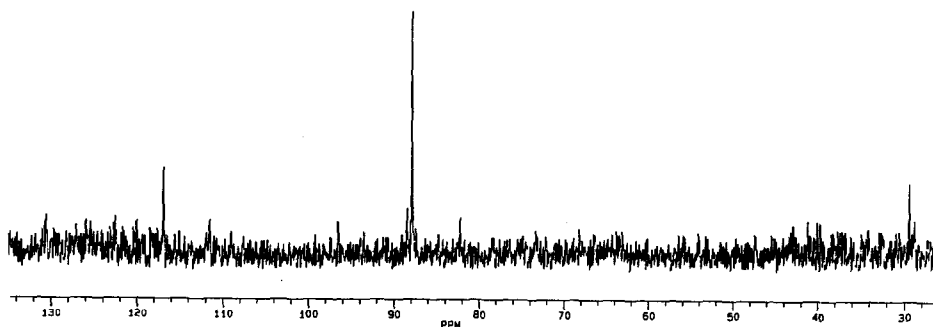
Previous results<sup>8,9</sup>, suggested that compound (1) exists as a single conformer in DMSO and methanol solution. However, the two papers gave different assignments to the various <sup>1</sup>H and <sup>13</sup>C resonances, and hence arrived at different conformations. Imanishi *et al.* suggested a conformation of type D (Figure 1) in which the imidazole ring is folded back over the diketopiperazine ring<sup>9</sup>. Jackson *et al.* however determined a structure of type B (Figure 1) in which the phenyl ring is folded back over the diketopiperazine<sup>8</sup>. However, examination of the 250MHz NMR spectrum dipeptide (1) in DMSO-d<sub>6</sub> (Figure 2a) showed both of these analyses to be incomplete. In addition to the expected resonances, a number of additional peaks of lesser intensity could be seen. Indeed almost every resonance was duplicated although sometimes at very different chemical shifts, indicating the presence of two distinct conformations. The corresponding spectrum in CD<sub>3</sub>OD (Figure 2b) was less convincing due to the lower solubility of compound (1) in CD<sub>3</sub>OD. However, again evidence could be found for the presence of a second conformer due to the presence of a number of minor peaks.

Figure 2: <sup>1</sup>H NMR Spectrum of Compound (1) a) in DMSO-d<sub>6</sub>, b) in CD<sub>3</sub>OD.



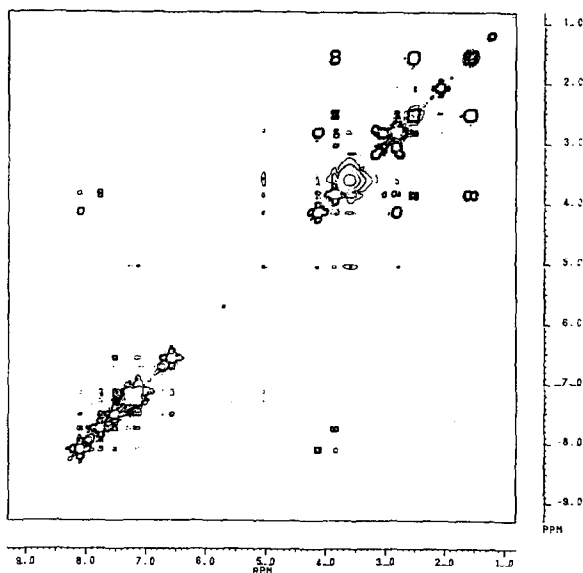
In view of the discrepancies in the literature<sup>8,9</sup>, it was necessary to unambiguously assign each of the major peaks in the  $^1\text{H}$  nmr spectrum before any conformational information could be obtained. This was done by the use of two complementary and independent techniques, long range  $^1\text{H}$ - $^{13}\text{C}$  correlation, and NOSEY. The crucial correlation in the long range (optimised for 2 and 3 bond couplings)  $^1\text{H}$ - $^{13}\text{C}$  correlation was a cross peak between the proton resonance at 1.55 ppm, and the carbon resonance at 117.5 ppm. This carbon resonance (which a DEPT spectrum showed to be quaternary) can be unambiguously assigned to C4 of the imidazole ring, thus the proton resonance at 1.55 ppm must be one of the diastereotopic histidine  $\beta$ -protons. The key cross section is shown in Figure 3. Once this proton had been assigned, all of the other proton resonances could be assigned by a COSY spectrum (Figure 4). This showed that the previous assignments of Jackson *et al.* were mainly correct<sup>8</sup>, but that the imidazole and amide protons had been misassigned.

Figure 3: Cross Section of the Long Range  $^1\text{H}$ - $^{13}\text{C}$  Correlation of Compound (1) at 1.55ppm.



The peak at 30 ppm corresponds to the histidine  $\beta$ -carbon, that at 88 ppm to a band of noise, and that at 117.5 ppm to C4 of the imidazole ring.

Figure 4: A  $^1\text{H}$ - $^1\text{H}$  Correlation Spectrum of Compound (1) in DMSO.



From Figure 4, it can be seen that the peaks at 6.57 and 7.52 ppm (and the minor resonance at 6.71 ppm) are due to the imidazole CH's, not to NH's as previously assigned. The histidine amide NH resonance occurs at 7.76 ppm, whilst the phenylalanine amide NH resonance occurs at 8.10 ppm with a minor peak at 7.96 ppm. These peaks had previously been assigned to the imidazole protons.

These assignments were confirmed by a NOSEY spectrum, in which the protons at 1.55 ppm and 2.51 ppm showed correlations to the peak at 6.57 ppm corresponding to H5 of the imidazole. Thus these two protons could be assigned to the diastereotopic histidine  $\beta$ -protons. The protons resonating at 2.8 ppm ( $\text{PhCH}_2$ ) showed no correlation to H5 of the imidazole. Thus these results are in complete agreement with those obtained by heteronuclear correlation, and the proton resonances of compound (1) have thus been unambiguously assigned by two independent methods.

Probably the most striking feature of the  $^1\text{H}$  NMR spectrum of compound (1) is the unusual chemical shift (1.55 ppm) observed for one of the histidine protons. (The other histidine proton resonance occurs at 2.51 ppm which is a more normal position for this type of proton). The explanation for this unusual chemical shift as proposed previously<sup>8</sup>, and also indicated by the modelling studies presented here is that the phenyl ring is folded over the diketopiperazine ring resulting in the shielding of one of the histidine  $\beta$ -protons. This is best seen in a space filling model as shown in Figure 5, the  $\text{CD}_3\text{OD}$  spectrum also shows this unusual chemical shift (1.84 ppm) for the same proton. The observed coupling constants between the  $\alpha$  and  $\beta$  protons of the major conformer of compound (1) in both  $\text{DMSO}-d_6$  and  $\text{CD}_3\text{OD}$  are also generally in agreement with those predicted for the conformation shown in Figure 5 as shown in Table 4. Thus it appears that the structure shown in Figure 5 represents the basic structure of the major conformation of compound (1) present in solution. This type of conformation has previously been proposed for other diketopiperazines with an aromatic side chain<sup>13</sup>.

Figure 5: A Space Filling Model of the Global Minimum Energy Conformation of Compound (1).



Table 4: Predicted and Observed Coupling Constants for the Major Diastereomer.

	PHE CH <sub>α</sub> -CH <sub>β1</sub> <sup>2</sup>	PHE CH <sub>α</sub> -CH <sub>β2</sub>	HIS CH <sub>α</sub> -CH <sub>β1</sub>	HIS CH <sub>α</sub> -CH <sub>β2</sub>
Observed DMSO	4.6 Hz	4.6 Hz	8.7 Hz	3.5 Hz
Observed CD <sub>3</sub> OD	4.7 Hz	3.8 Hz	7.6 Hz	5.0 Hz
Predicted <sup>1</sup> Vacuum	3.8 Hz	2.8 Hz	11.1 Hz	1.7 Hz
Predicted CHCl <sub>3</sub>	3.7 Hz	2.7 Hz	11.0 Hz	1.6 Hz
Predicted Water	4.0 Hz	2.8 Hz	11.6 Hz	3.5 Hz

1) Values obtained from the Macromodel 3-D programme. The values are a weighted average of the coupling constants calculated for each conformer of type B with a flat diketopiperazine ring. 2) For phenylalanine β1 represents the proton visible in Figure (5); for histidine, β1 is the highly shielded proton visible in Figure (5). In both cases β2 represents the diastereotopic proton.

Although the NMR spectra of compound (1) in DMSO-d<sub>6</sub> and CD<sub>3</sub>OD are generally similar (Figure 2), showing only small (<0.3 ppm) differences in chemical shift, there is a significant difference in the imidazole CH resonances. These two peaks both occur at a much lower field in CD<sub>3</sub>OD (6.94 and 8.75 ppm) than in DMSO-d<sub>6</sub> (6.52 and 7.51 ppm). This is consistent with a change from an intramolecularly hydrogen bonded structure in DMSO as shown in Figure 5 to a none hydrogen bonded structure in methanol. Thus for the major conformer of dipeptide (1), the observed NMR spectra are in excellent agreement with the structure predicted by molecular mechanics.

Little information about the structure of the minor conformer could be obtained from the room temperature <sup>1</sup>H NMR spectrum due to overlap of the peaks for this conformer with those for the major conformer, and for HOD. In order to overcome this problem, and to obtain information on the dynamic behaviour of compound (1), a variable temperature NMR study was undertaken.

#### Variable Temperature NMR Results

The <sup>1</sup>H NMR spectrum of dipeptide (1) in DMSO-d<sub>6</sub> was recorded in 10°C increments from 30°C to 140°C. Throughout this temperature range, there was no change in the chemical shift of the imidazole CH protons, but the multiplet at 7.1-7.4 ppm corresponding to the phenyl protons underwent considerable simplification as the temperature was raised, although it remained a multiplet at 140°C. The amide NH resonances gradually merged into a single resonance by 100°C, and disappeared completely by 130°C. The results for the remaining peaks are tabulated in Table 5. From the data in Table 5, the following conclusions can be reached for the major conformer:-

The chemical shift of the His α-CH resonance increases slightly as the temperature increases (1.7 x 10<sup>-3</sup> ppm/°C). The coupling constants do not change over the temperature range, although the resolution increases as the temperature increases, so that at high temperature an additional 1.1 Hz coupling is visible. These results indicate that the histidine residue does not change its conformation on raising the temperature (no change in coupling constants). The small change in chemical shift may be due to a change in the conformation of the phenylalanine residue *vide infra*. The 1.1 Hz coupling is a cross ring coupling to the Phe α-CH, and indicates that the diketopiperazine ring is essentially flat as predicted by molecular modelling<sup>14</sup>.

For both His β-CH<sub>2</sub>'s, the chemical shift increases as the temperature increases (5.9 x 10<sup>-3</sup> ppm/°C for the higher field proton and 3.0 x 10<sup>-3</sup> ppm/°C for the lower field proton), but there is no change in any of the



Table 5: Variable Temperature NMR data 22-140°C in DMSO *d*<sub>6</sub>

Temp. °C	Major Conformer			Minor Conformer		
	Phe-CH <sub>α</sub>	His-CH <sub>α</sub>	Phe-CH <sub>2β</sub>	His-CH <sub>2β</sub>	Phe-CH <sub>α</sub>	His-CH <sub>2β</sub>
140	4.16ppm td J 5.5, 1.0	4.02ppm ddd J 8.5, 4.0, 1.0	2.96ppm multiplet	2.86ppm dd J 14.9, 4.2	3.97ppm t J 5.3	3.53ppm t J 5.3
130	4.16ppm td J 5.5, 1.0	4.01ppm ddd J 8.5, 4.0, 1.1	2.95ppm multiplet	2.84ppm dd J 15.0, 3.9	3.96ppm t J 5.7	3.50ppm dd J 7.1, 4.2
120	4.16ppm td J 5.5, 1.1	3.99ppm ddd J 8.5, 4.0, 1.1	2.93ppm multiplet	2.81ppm dd J 14.9, 4.0	3.95ppm td J 5.3, 0.8	3.47ppm ddd J 7.2, 4.2, 0.8
110	4.15ppm td J 5.5, 1.1	3.98ppm ddd J 8.5, 4.0, 1.1	2.92ppm multiplet	2.79ppm dd J 14.9, 4.0	3.94ppm t J 4.5	3.44ppm ddd J 7.2, 4.2, 0.8
100	4.15ppm t J 5.5	3.97ppm dd J 8.5, 3.6	2.91ppm multiplet	2.77ppm dd J 14.8, 4.0	3.93ppm t J 5.3	3.02ppm dd J 11.5, 5.1
90	4.15ppm t J 5.4	3.96ppm dd J 8.6, 3.6	2.90ppm multiplet	2.75ppm dd J 14.9, 4.0		3.02ppm dd J 14.8, 5.0
80	4.14ppm t J 5.1	3.94ppm dd J 8.7, 4.1	2.89ppm multiplet	2.72ppm dd J 14.8, 3.9	2.97ppm multiplet	2.83ppm multiplet
70	4.14ppm t J 4.9	3.93ppm dd J 8.6, 3.7	2.87ppm multiplet	2.69ppm dd J 14.7, 4.0	2.94ppm multiplet	2.81ppm multiplet
60	4.14ppm t J 4.8	3.91ppm unresolved	2.86ppm d J 5.0	2.66ppm dd J 14.6, 3.9	2.93ppm multiplet	2.76ppm dd J 15.0, 6.7
40	4.14ppm unresolved	3.86ppm unresolved	2.84ppm d J 4.8	2.59ppm dd J 14.5, 3.2	3.23ppm unresolved	2.75ppm dd J 14.9, 6.1
30	4.14ppm unresolved	3.85ppm unresolved	2.83ppm d J 4.8	2.56ppm dd J 14.6, 3.9	3.19ppm unresolved	2.75ppm multiplet
22	4.12ppm unresolved	3.82ppm unresolved	2.80ppm d J 4.6	2.51ppm dd J 14.5, 3.5	3.17ppm unresolved	2.75ppm unresolved

A space indicates that the resonance was hidden either under the water peak, or under other resonances. Quoted coupling constants are as they appear in the spectrum, and have not been corrected for second order effects. The Phe-CH<sub>2β</sub> peaks for both the major and minor conformer appear as one resonance corresponding to both protons. For most of the temperature range these peaks appear as a pseudo doublet. In reality they must be two highly second order dd's with the outer peaks lost amongst the other peaks. For most of the temperature range, the high field His-CH<sub>2β</sub> proton of the minor conformer is only partially visible beneath other peaks. In these cases, it is given a chemical shift but no coupling constants.

coupling constants. The absence of any change in any of the coupling constants again indicates that the histidine residue does not change its conformation over the temperature range. However, the large change in the chemical shifts indicates that these protons become less shielded as the temperature increases. This can be explained by assuming that at elevated temperatures, the phenylalanine residue spends a greater proportion of time in non-folded conformations. As would be expected for this hypothesis, the higher field proton which is more shielded by the phenyl ring is the one which undergoes the largest change in chemical shift.

The Phe  $\alpha$ -CH shows no change in chemical shift or coupling constant as the temperature increases, although the resolution improves with temperature so that at high temperature a 1.1Hz cross ring coupling to the His  $\alpha$ -CH can be seen.

The resonances corresponding to the Phe  $\beta$ -CH<sub>2</sub>'s, undergo complex changes as the temperature increases. There is a small increase in chemical shift ( $1.4 \times 10^{-3}$  ppm/°C) though this may be due to the changes in the coupling pattern. At room temperature, the two protons are accidentally equivalent resulting in a doublet; however, as the temperature increases they cease to be identical and the coupling undergoes a number of changes. However, the two resonances never completely separate, and the observed coupling constants must be treated with caution, thus no conclusions can be drawn from them. The fact that the coupling pattern does change as the temperature changes, however, does indicate that the conformation of the phenylalanine residue changes with temperature and is consistent with the results obtained for the His  $\beta$ -protons, and from molecular modelling.

This variable temperature study was also extended to low temperature (10° C increments from 20° C to -80° C) by studying the spectrum of compound (1) dissolved in CD<sub>3</sub>OD. The results were not as useful as the higher temperature spectra, as at low temperature extensive line broadening occurs. Throughout the low temperature range, the only significant change in the aromatic region of the nmr spectrum was that H2 of the imidazole shifted from 8.75ppm at 20° C to 9.0ppm at -80° C. This is consistent with an increase in hydrogen bonding at lower temperatures.

The His  $\alpha$ -CH resonance undergoes a small shift to higher field as the temperature decreases (4.05ppm at 20° C to 3.94ppm at -80° C), this is entirely consistent with the high temperature results for this resonance. At 20° C, this peak occurs as a ddd (*J* 7.8, 5.0, 1.3Hz) and these coupling constants are consistent with those observed in DMSO-*d*<sub>6</sub>. The 1.3Hz coupling is a <sup>5</sup>*J* cross ring coupling to the Phe  $\alpha$ -CH and indicates that the diketopiperazine ring is again flat.

Of the two His  $\beta$ -CH<sub>2</sub> resonances, the highly shielded proton (1.92ppm, dd, *J* 15.0, 7.6Hz at 20° C) undergoes a considerable shift to higher field as the temperature is decreased (0.68ppm, unresolved at -80° C). The rate of change of chemical shift of this proton ( $1.2 \times 10^{-2}$  ppm/°C) is approximately double the rate at which the chemical shift of the corresponding proton increases in DMSO-*d*<sub>6</sub>. This indicates that at room temperature the phenyl ring is not locked over the diketopiperazine, but is rotating about the C <sub>$\alpha$</sub> -C <sub>$\beta$</sub>  bond. Such a rotation would also account for the observed CH <sub>$\alpha$</sub> -CH <sub>$\beta$ 1</sub> coupling constants being smaller than predicted for a folded conformer (Table 4). Even at -80° C there is no reason to suppose that this rotation is completely suppressed as there is a considerable change in the chemical shift of this proton (0.06ppm) between -70° C and -80° C. The other His  $\beta$ -CH<sub>2</sub> proton undergoes no change in chemical shift as the temperature decreases, staying at 2.51ppm. At 20° C this resonance occurs as a dd (*J* 15.0, 7.6Hz), so both His  $\beta$ -CH<sub>2</sub> protons show comparable coupling constants in DMSO-*d*<sub>6</sub>, and CD<sub>3</sub>OD, again indicating that the same conformation is adopted in both solvents.

The Phe  $\alpha$ -CH shows a small increase in chemical shift as the temperature decreases (4.37ppm at 20°C to 4.49ppm at -80°C) and the resolution decreases from a ddd (J 4.8, 3.8, 1.2Hz) at 20°C to a broad singlet at -80°C. Again these results are entirely compatible with those observed in DMSO- $d_6$  and for the His peaks in CD<sub>3</sub>OD. The Phe  $\beta$ -CH<sub>2</sub> protons again show a single resonance (a multiplet at 2.97ppm) and this does not change with temperature.

In summary, these results indicate that at room temperature in DMSO, dipeptide (1) exists predominantly in the folded conformation shown in Figure 5<sup>13</sup>. As the temperature increases however, the phenylalanine residue spends a greater proportion of time in non-folded conformations obtained by rotation about the C $\alpha$ -C $\beta$  bond and predicted by molecular modelling, and as the temperature decreases it spends less time in these conformations. Interconversion between these conformers must be rapid as only a single set of resonances are observed by NMR. The histidine residue is essentially rigid (possibly due to an intramolecular hydrogen bond) and does not undergo any conformational changes at elevated temperature.

#### *The Minor Conformer*

Unlike the major conformer, the <sup>1</sup>H nmr spectrum of the minor conformer in  $d_6$ -DMSO or CD<sub>3</sub>OD shows no unusual chemical shifts, indicating that no proton is in an unusually shielded position. This would fit a conformation of type A or C found by molecular modelling. A comparison of the observed CH $\alpha$ -CH $\beta$  coupling constants with those calculated for conformations of type A and C as shown in Table 6, clearly indicates that the minor conformer has a structure of type A with the two aromatic rings facing one another. This type of conformation has previously been found for a variety of diketopiperazines derived from two aromatic amino acids, and is thought to be stabilised by  $\pi$ - $\pi$  interactions between the two aromatic rings<sup>15</sup>.

*Table 6: Observed and Predicted Coupling Constants for Conformations of Types A and C*

	PHE CH $\alpha$ -CH $\beta$	HIS CH $\alpha$ -CH $\beta$
Predicted <sup>1</sup> Vacuum Type A	2.0, 4.8	2.9, 3.4
Predicted Vacuum Type C	2.9, 11.8	1.8, 11.4
Predicted Chloroform Type A	3.0, 3.3	1.7, 5.4
Predicted Chloroform Type C	1.8, 11.4	3.1, 11.8
Predicted Water Type A	3.0, 3.3	2.8, 3.9
Predicted Water Type C	2.7, 3.7	3.1, 11.8
<u>Observed<sup>2</sup></u>	<u>both 4.5-5.7</u>	<u>4.0-5.1, 5.5-7.1</u>

1) Predicted coupling constants are a weighted average for all conformers of that type found by the molecular modelling at 298.15K. Values are calculated within the Macromodel program. 2) The observed coupling constants are given as a range of values obtained from the H $\alpha$  or H $\beta$  resonances at various temperatures.

The variable temperature nmr results presented in Table 5 show that this conformation undergoes only very minor changes on raising the temperature. The chemical shift of the His  $\alpha$ -CH resonance increases slightly as the temperature increases ( $3.1 \times 10^{-3}$  ppm/°C), and the peak becomes better resolved so that at higher temperatures all the coupling constants including a cross ring coupling of 0.8 Hz to the Phe  $\alpha$ -CH can be determined. The magnitude of this coupling constant indicates that the diketopiperazine ring is essentially

flat as predicted by the molecular modelling<sup>14</sup>. The improvement in resolution as the temperature increases can be explained by assuming that more than one conformation of type A exists, and that as the temperature increases the rate of exchange between these increases. This also explains the small change in chemical shift as the populations of the two or more conformations will vary with temperature.

Of the two His  $\beta$ -CH's, one undergoes a small increase in chemical shift as the temperature increases ( $1.25 \times 10^{-3}$  ppm/°C), whilst the other remains unchanged. The coupling constants undergo no change as the temperature varies, again indicating the absence of any major conformational change.

The Phe  $\alpha$ -CH only becomes visible from beneath the water resonance at 100°C, and it then undergoes a very small increase in chemical shift as the temperature increases ( $1.0 \times 10^{-3}$  ppm/°C) although the small temperature range over which this peak could be observed means that this is within the experimental error. The two Phe  $\beta$ -CH's, appear as a single resonance which becomes better resolved and increases in chemical shift slightly as the temperature increases ( $1.5 \times 10^{-3}$  ppm/°C) again indicating only minor conformational changes.

No useful information concerning the minor conformation could be obtained from the low temperature nmr study in CD<sub>3</sub>OD owing to the low solubility and low resolution observed for these spectra. In summary, the molecular modelling and variable temperature nmr results indicate that the minor conformer of dipeptide (1) has a structure of type A, and that this changes only slightly over the temperature range of 22-140°C.

### *<sup>13</sup>C NMR Results*

The <sup>13</sup>C nmr spectrum of dipeptide (1) was recorded both in solution and in the solid state. The solution spectrum (fully decoupled and DEPT in DMSO-*d*<sub>6</sub>) showed all of the expected signals doubled up, again indicating the presence of two conformations. The full assignments are:- 30.80, and 31.39 (2x His-CH<sub>2</sub>), 39.16, and 39.49 (2x Phe-CH<sub>2</sub>), 53.82, 54.49, 55.46, and 55.48 (4x  $\alpha$ -CH), 117 (broad, imidazole-C), 126.83, 128.19, 128.33, 130.19, and 130.31 (5x ArCH), 135.13 (imidazole-CH), 136.08, and 136.31 (2x ArC), 166.35, 166.86, 167.24, and 167.46 (4x CO). Other than providing further evidence for the presence of two slowly interconverting conformers, no conformational information could be obtained from the <sup>13</sup>C spectrum, as no unusual chemical shifts were obtained. A CPMAS solid state <sup>13</sup>C spectrum was also obtained, this showed very broad lines, at the same chemical shifts as the solution spectra. (The resolution was too poor to separate the individual conformers if they exist in the solid state.)

### *Conclusions*

The cyclic dipeptide (1) exists in both DMSO and methanol solutions as a mixture of two slowly interconverting conformers. The major conformer has a folded shape with the phenyl group folded over the diketopiperazine (Figure 1 Type B, Figure 5). The imidazole is essentially rigid being held in place by an intramolecular hydrogen bond between H3 of the imidazole and the histidine carbonyl. The phenyl ring however is rotating about the  $\alpha$ - $\beta$  bond with the folded conformation simply being the global minimum of a set of conformations. The rate of rotation is temperature dependant over the range -80°C to +140°C as shown by the shielding experienced by the histidine  $\beta$ -protons.

The minor conformer is U shaped (Figure 1 Type A) with the two aromatic rings facing one another. The imidazole is held in position by an intramolecular hydrogen bond between H3 of the imidazole and the

histidine carbonyl, and variable temperature nmr studies showed no evidence of any rotation about the phenylalanine  $\alpha$ - $\beta$  bond.

Both types of conformation were predicted by a molecular modelling study which in chloroform indicated that the ratio of the major diastereomer to the minor one (Type B+C/A) should be approximately 8:1 and this is indeed observed by nmr. However the modelling study also predicted the presence of an additional class of conformer (Type D) for which no evidence was obtained by nmr.

Further studies on the catalytically active conformation of diketopiperazine (1) and related cyclic dipeptides are in progress and will be reported in due course.

### Experimental

Diketopiperazine (1) was prepared by the literature procedure<sup>6</sup>, and recrystallised from methanol. All nmr spectra were obtained on a Bruker AM250 spectrometer fitted with a 5mm  $^1\text{H}/^{13}\text{C}$  dual probe. Proton nmr spectra and  $^1\text{H}$ - $^1\text{H}$  correlations were recorded at a concentration of c.a. 10mg in 0.5ml of solvent.  $^{13}\text{C}$  spectra and  $^1\text{H}$ - $^{13}\text{C}$  correlations were recorded on saturated solutions. The  $^{13}\text{C}$  CPMAS spectrum was recorded on the same spectrometer fitted with a solid state probe, and using c.a. 250mg of sample. All resonances are reported in ppm downfield of external TMS and are referenced to the residual solvent peak.

### Acknowledgements

The author would like to thank Mr. E. Lewis for his assistance with the nmr work, and the Wolfson foundation for providing the funds to purchase the Silicon Graphics Molecular Modelling Workstation. Financial support for this project was provided by the University of Wales at Bangor.

### References

1. Mowry, D.T. *Chem. Rev.*, **1948**, 42, 189.
2. Jackson, W.R.; Jacobs, H.A.; Jayatilake, G.S.; Matthews, B.R.; Watson, K.G. *Aust. J. Chem.*, **1990**, 43, 2045; Effenberger, F.; Stelzer, U. *Angew. Chem., Int. Ed. Engl.*, **1991**, 30, 873; Watson, K.G.; Fung, Y.M.; Gredley, M.; Bird, G.J.; Jackson, W.R.; Gountzos, H.; Matthews, B.R. *J. Chem. Soc., Chem. Commun.*, **1990**, 1018; Jackson, W.R.; Jacobs, H.A.; Matthews, B.R.; Jayatilake, G.S.; Watson, K.G. *Tetrahedron Lett.*, **1990**, 31, 1447; Matthews, B.R.; Gountzos, H.; Jackson, W.R.; Watson, K.G. *Tetrahedron Lett.*, **1989**, 30, 5157.
3. Bredig, G.; Fiske, P.S. *Biochem. Z.*, **1912**, 46, 7; Bredig, G.; Minaeff, M. *Biochem. Z.*, **1932**, 249, 16.
4. Tsuboyama, S. *Bull. Chem. Soc. Jpn.*, **1965**, 38, 354; Danda, H.; Chino, K.; Wake, S. *Chem. Lett.*, **1991**, 731; Tsuboyama, S. *Bull. Chem. Soc. Jpn.*, **1966**, 39, 698; Tsuboyama, S. *Bull. Chem. Soc. Jpn.*, **1962**, 35, 1004.
5. Mori, A.; Nitta, H.; Kudo, M.; Inoue, S. *Tetrahedron Letts*, **1991**, 32, 4333; Mori, A.; Ohno, H.; Nitta, H.; Tanaka, K.; Inoue, K. *Synlett*, **1991**, 563; Minamikawa, H.; Hayakawa, S.; Yamada, T.; Iwasawa, N.; Narasaka, K. *Bull. Chem. Soc. Jpn.*, **1988**, 61, 4379; Narasaka, K.; Yamada, T.; Minamikawa, H. *Chem. Lett.*, **1987**, 2073; Reetz, M.T.; Kunisch, F.; Heitmann, P. *Tetrahedron Letts.*, **1986**, 27, 4721; Hayashi, M.; Matsuda, T.; Oguni, N. *J. Chem. Soc., Chem. Commun.*, **1990**, 1364; Kobayashi, S.; Tsuchiya, Y.; Mukaiyama, T. *Chem. Lett.*, **1991**, 541.

6. Kobayashi, Y.; Asada, S.; Watanabe, I.; Hayashi, H.; Motoo, Y.; Inoue, S. *Bull. Chem. Soc. Jpn.*, **1986**, 59, 893; Kobayashi, Y.; Hayashi, H.; Miyaji, K.; Inoue, S. *Chem. Lett.*, **1986**, 931; Oku, J.-I.; Inoue, S. *J. Chem. Soc., Chem. Commun.*, **1981**, 229; Mathews, B.R.; Jackson, W.R.; Jayatilake, G.S.; Wilshire, C.; Jacobs, H.A. *Aust. J. Chem.*, **1988**, 41, 1697; Asada, S.; Kobayashi, Y.; Inoue, S. *Makromol. Chem.*, **1985**, 186, 1755; Danda, H.; Nishikawa, H.; Otaka, K. *J. Org. Chem.*, **1991**, 56, 6740; Danda, H. *Synlett.*, **1991**, 263.
7. Tanaka, K.; Mori, A.; Inoue, S. *J. Org. Chem.*, **1990**, 55, 181; Oku, J.-I.; Ito, N.; Inoue, S. *Makromol. Chem.*, **1982**, 183, 579.
8. Jackson, W.R.; Jayatilake, G.S.; Matthews, B.R.; Wilshire, C. *Aust. J. Chem.*, **1988**, 41, 203.
9. Masuda, Y.; Tanihara, M.; Imanishi, Y.; Higashimura, T. *Bull. Chem. Soc. Jpn.*, **1985**, 58, 497.
10. Arlt, D.; Jautelat, M.; Lantzsch, R. *Angew.Chem., Int. Ed. Engl.*, **1981**, 20, 703.
11. Ognyanov, V.I.; Datcheva, V.K.; Kyler, K.S. *J. Am. Chem. Soc.*, **1991**, 113, 6992; Van-Scharrenburg, G.J.M.; Sloothaak, J.B. *Recueil des Travaux Chimiques des Pays-Bas*, **1991**, 110, 209; Zandbergen, P.; Van der Linden, J.; Brussee, J.; Van der Gen, A. *Synth. Commun.*, **1991**, 21, 1387; Effenberger, F.; Horsch, B.; Weingart, F.; Ziegler, T.; Kuhner, S. *Tetrahedron Letts.*, **1991**, 32, 2605; Becker, W.; Freund, H.; Pfeil, E. *Angew. Chem., Int. Ed. Engl.*, **1965**, 4, 1079; Becker, W.; Pfeil, E. *J. Am. Chem. Soc.*, **1966**, 88, 4299; Ziegler, T.; Horsch, B.; Effenberger, F. *Synthesis*, **1990**, 575; Becker, W.; Pfeil, E. *Biochemische Zeitschrift*, **1966**, 346, 301.
12. Still, W.C.; Mohmadi, F.; Richards, N.G.J.; Guida, W.C.; Lipton, M.; Liskamp, R.; Chang, G.; Hendrickson, T.; DeGunst, F.; Hasel, W. *Macromodel 3D.*, Version 3.1, Columbia Univesrsity, New York, NY, **1991**.
13. Sheinblatt, M. *Int. J. Peptide Protein Res.*, **1991**, 38, 8; Kojima, Y.; Yamashita, T.; Nishide, S.; Hirotsu, K.; Higuchi, T. *Bull. Chem. Soc. Jpn.*, **1985**, 58, 409; Kopple, K.D.; Marr, D.H. *J. Am. Chem. Soc.*, **1967**, 89, 6193; Sheinblatt, M. *J. Chem. Soc., Perkin Trans. II*, **1990**, 127; Kopple, K.D.; Ohnishi, M. *J. Am. Chem. Soc.*, **1969**, 91, 962; Ziauddin; Kopple, K.D. *J. Org. Chem.*, **1970**, 35, 253; Lin, C.F.; Webb, L.E. *J. Am. Chem. Soc.*, **1973**, 95, 6803; Arena, G.; Impellizzeri, G.; Maccarrone, G.; Pappalardo, G.; Sciotto, D.; Rizzarelli, E. *J. Chem. Soc., Perkin Trans. 2*, **1992**, 371; Arena, G.; Impellizzeri, G.; Maccarrone, G.; Pappalardo, G.; Sciotto, D.; Rizzarelli, E. *Thermochimica Acta*, **1989**, 154, 97; Sheinblatt, M.; Andorn, M.; Rudi, A. *Int. J. Peptide Protein Res.*, **1988**, 31, 373; Tanihara, M.; Imanishi, Y.; Higashimura, T. *Biopolymers*, **1977**, 16, 2217.
14. Davies, D.B.; Khaled, Md. A. *J. Chem. Soc., Perkin Trans. II*, **1976**, 1238.
15. Deslauriers, R.; Grzonka, Z.; Schaumburg, K.; Shiba, T.; Walter, R. *J. Am. Chem. Soc.*, **1975**, 97, 5093.